J|A|C|S
ARTICLES
Published on Web 02/04/2006

Evidence for Two Forms, Double Hydrogen Tunneling, and Proximity of Excited States in Bridge-Substituted Porphycenes: Supersonic Jet Studies

Alexander Vdovin, Jerzy Sepioł,* Natalia Urbańska, Marek Pietraszkiewicz, Andrzej Mordziński,[1] and Jacek Waluk*

Contribution from the Photochemistry and Spectroscopy Department and Laser Centre, Institute of Physical Chemistry, Polish Academy of Sciences, Kasprzaka 44/52, 01-224 Warsaw, Poland

Received August 8, 2005; E-mail: waluk@ichf.edu.pl

Abstract: Laser-induced fluorescence and dispersed fluorescence spectra measured in supersonic jets for 9,10,19,20-tetra-*n*-methylporphycene and 9,10,19,20-tetra-*n*-propylporphycene reveal, for both compounds, the presence of two different species which are assigned to trans and cis tautomeric forms. Doublet splitting of lines is observed, disappearing upon deuteration of the inner nitrogen atoms. This finding is interpreted as an indication of double hydrogen tunneling. The values of tunneling splitting are obtained for both ground and lowest singlet excited states. The splitting is similar for cis and trans forms, and the barrier for tautomerization is larger in the excited state. Due to the coupling of hydrogen motion with rotation of alkyl substituents, tautomerization occurs in an asymmetric double minimum potential, with the ordering of energy minima reversed upon excitation. The second singlet excited state is found to lie very close to S_1, thus facilitating an efficient radiationless depopulation.

Introduction

Synthesis of porphycene (**1**),[2] a constitutional isomer of porphyrin (**2**), opened many new possibilities in porphyrin-related areas of research.[3] Even though general structural and spectral patterns are qualitatively similar in the two isomers, quantitative differences may sometimes be immense. For instance, the lowest electronic transition (Q-band) in porphycene is more than an order of magnitude stronger than that in porphyrin and also significantly red-shifted. Such a pattern, combined with other photophysical characteristics, makes porphycene a potentially much better agent for photodynamic therapy than parent porphyrin and its derivatives. This prediction has been firmly corroborated, using various substituted porphycenes in the treatment of tumors[4] and in photoinactivation of bacterial strains.[5]

Large differences between **1** and **2** have also been revealed in the rates and mechanisms of intramolecular tautomerization (Chart 1). The two inner hydrogen atoms can migrate back and forth between the four nitrogen atoms that constitute the inner cavity. This process has been thoroughly studied for **2**, mostly by NMR spectroscopy.[6−8] There is no doubt that the most stable tautomeric form in porphyrin is of trans type, with protons localized on the opposite nitrogen atoms. The interconversion between two equivalent trans tautomers in the ground state is strongly temperature-dependent: the reported rate at 298 K is larger than 2×10^4 s^{-1}, whereas below 230 K the tautomerization is stopped[6] (it can still be photoinduced even at liquid helium temperatures,[9−11] albeit with a rather small quantum yield). The mechanism of the ground-state reaction involves a stepwise process, with the first hydrogen atom tunneling to the cis form, in which the protons are located on adjacent nitrogen atoms. The level from which the tunneling occurs has to be thermally activated. The energy required for the tunneling (24.0 kJ/mol[6]) comprises contributions due to (a) cis−trans energy difference and (b) reorganization energy of the molecular skeleton. After achieving the cis configuration, the system can

(1) Deceased October 5, 2004.
(2) Vogel, E.; Köcher, M.; Schmickler, H.; Lex, J. *Angew. Chem., Int. Ed. Engl.* **1986**, *25*, 257.
(3) Sessler, J. L.; Gebauer, A.; Vogel, E. Porphyrin Isomers. In *The Porphyrin Handbook*; Kadish, K. M., Smith, K. M., Guilard, R., Eds.; Academic Press: San Diego, CA, 2000; Vol. 2, p 1.
(4) (a) Richert, C.; Wessels, J. M.; Müller, M.; Kisters, M.; Benninghaus, T.; Goetz, A. E. *J. Med. Chem.* **1994**, *37*, 2797. (b) Gottfried, V.; Davidi, R.; Averbuj, C.; Kimel, S. *J. Photochem. Photobiol., B* **1995**, *30*, 115. (c) Szeimies, R. M.; Karrer, S.; Abels, C.; Steinbach, P.; Fickweiler, S.; Messmann, H.; Bäumler, W.; Landtaler, M. *J. Photochem. Photobiol., B* **1996**, *34*, 67. (d) Villanueva, A.; Cañete, M.; Nonell, S.; Borrell, J. I.; Teixidó, J.; Juarranz, A. *Anti-Cancer Drug Des.* **1996**, *11*, 89. (e) Abels, C.; Szeimies, R. M.; Steinbach, P.; Richert, C.; Goetz, A. E. *J. Photochem. Photobiol., B* **1997**, *40*, 305. (f) Karrer, S.; Abels, C.; Szeimies, R. M.; Bäumler, W.; Dellian, M.; Hohenleutner, U.; Goetz, A. E.; Landthaler, M. *Arch. Dermatol. Res.* **1997**, *289*, 132. (g) Mak, N. K.; Kok, T. W.; Wong, R. N. S.; Lam, S. W.; Lau, Y. K.; Leung, W. N.; Cheung, N. H.; Huang, D. P.; Yeung, L. L.; Chang, C. K. *J. Biomed. Sci.* **2003**, *10*, 418. (h) Cañete, M.; Ortega, C.; Gavaldá, A.; Cristobal, J.; Juarranz, A.; Nonell, S.; Teixidó, J.; Borrell, J. I.; Villanueva, A.; Rello, S.; Stockert, J. C. *Int. J. Oncol.* **2004**, *24*, 1221. (i) Scherer, K.; Abels, C.; Bäumler, W.; Ackermann, G.; Szeimies, R. M. *Arch. Dermatol. Res.* **2004**, *295*, 535.
(5) (a) Polo, L.; Segalla, A.; Bertoloni, G.; Jori, G.; Schaffner, K.; Reddi, E. *J. Photochem. Photobiol., B* **2000**, *59*, 152. (b) Lauro, F. M.; Pretto, P.; Covolo, L.; Jori, G.; Bertoloni, G. *Photochem. Photobiol. Sci.* **2002**, *1*, 468.
(6) Braun, J.; Schlabach, M.; Wehrle, B.; Köcher, M.; Vogel, E.; Limbach, H. H. *J. Am. Chem. Soc.* **1994**, *116*, 6593.
(7) Braun, J.; Limbach, H. H.; Williams, P. G.; Morimoto, H.; Wemmer, D. E. *J. Am. Chem. Soc.* **1996**, *118*, 7231.
(8) Schlabach, M.; Wehrle, B.; Rumpel, H.; Braun, J.; Scherer, G.; Limbach, H. H. *Ber. Bunsen-Ges. Phys. Chem.* **1992**, *96*, 821.
(9) Korotaev, O. N.; Personov, R. I. *Opt. Spectrosc.* **1972**, *32*, 479.
(10) Radziszewski, J. G.; Waluk, J.; Michl, J. *J. Mol. Spectrosc.* **1990**, *140*, 373.
(11) Radziszewski, J. G.; Waluk, J.; Michl, J. *Chem. Phys.* **1989**, *136*, 165.

10.1021/ja054745m CCC: $33.50

Chart 1. Porphycene (**1**) and Porphyrin (**2**)

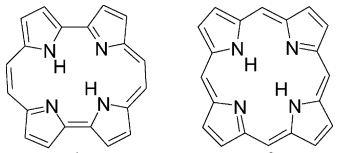

1 **2**

either return to the initial form or, via the transfer of the second hydrogen, end up as the other trans structure. Interestingly, the cis form, crucial for this mechanism, has never been experimentally detected, perhaps due to its short lifetime, of which the estimates range from less than 10 ps[12] to 10^{-8} s.[6]

Tautomeric properties of porphycene are totally different. The ground-state process is so fast that its rate could not be determined thus far. ^{15}N CPMAS NMR studies of crystalline **1** revealed that the tautomerization is extremely rapid even at 107 K.[13,14] Contrary to the case of **2**, the tautomerization in porphycene is also very efficient in the lowest excited singlet state. This is manifested by fluorescence depolarization.[15−17] Migration of the inner hydrogens leads to the change of the transition moment directions. As a result, the absolute values of the emission anisotropy become lower than those expected for a nontautomerizing molecule. Measurements of fluorescence anisotropy of **1** as a function of temperature showed that at 298 K the excited-state process is much faster than the fluorescence lifetime (about 10 ns), whereas at 20 K the reaction becomes too slow to compete with S_1 decay.[17] These studies have also unequivocally proved that the dominant form of porphycene is the trans tautomer, since depolarization would not occur for the case of cis−cis interconversion, whereas cis−trans or trans−cis processes would lead to smaller anisotropy changes than observed.

Differences between tautomeric properties of **1** and **2** are nicely reflected in the electronic spectra of samples isolated in supersonic jets. Fluorescence excitation spectra of porphycene reveal splitting of all the vibronic peaks into doublets separated by 4.4 cm^{-1}.[18] In singly and doubly deuterated species the splitting becomes too small to be detected (<1 cm^{-1}). This characteristic pattern of doublets, not observed in porphyrin,[19] was interpreted as a sign of tunneling splitting due to delocalization of two hydrogen atoms in a symmetrical double minimum potential, with a low energy barrier separating two trans forms. Evidence for ground-state tunneling was also obtained for a singly substituted derivative, 2,7,12,17-tetra-*n*-propyl-9-acetoxyporphycene, in condensed phases.[20] In this molecule, two ground-state trans tautomers, no longer equivalent, were observed at temperatures as low as 20 K.

The origin for completely different tautomeric behavior in the two isomers is due to different size and shape of the inner cavity formed by four nitrogen atoms. In porphyrin, the cavity is a square, with N−N separation of about 2.90 Å,[21] whereas in porphycene it has a rectangular shape, with N−N distances of 2.63 and 2.83 Å, respectively.[2] The former value corresponds to the hydrogen-bonded atoms. The shorter distance and a larger NH···N angle (152° in **1** versus 116° in **2**[14]) result in much stronger intramolecular hydrogen bonds in **1** and, thus, in a smaller barrier separating the two trans tautomers. The strength of the hydrogen bond in **1** with respect to that in **2** is also reflected in the calculations,[22] which predict that free base porphycene is more stable than porphyrin, whereas for metal derivatives the relative stabilities are reversed.

Chart 2. Porphycenes Studied in This Work and Their Possible Tautomeric Structures

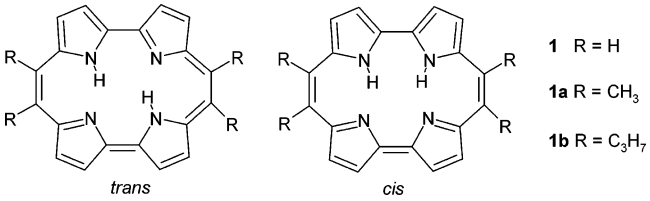

Another consequence of a shorter N−N distance is a decrease in the energy difference between the trans and cis forms. The calculations predict the cis tautomer in porphyrin to be less stable by about 8.5 kcal/mol than the trans structure,[23] whereas for porphycene this difference drops to about 2 kcal/mol.[22,24] It is known that alkyl substituents can strongly modulate the N−N separation in porphycenes. In particular, alkyl substitution on the ethylene bridges (positions 9, 10, 19, and 20) shortens this distance by as much as 0.1 Å.[25] Therefore, one could hope that in the meso-alkylated porphycenes the elusive cis species has a chance of being detected. Indeed, the B3LYP/6-31G(d,p) structure optimizations for the tetramethyl derivative predicted nearly isoenergetic cis and trans forms. More important, our initial studies in solutions and glasses revealed a doubly exponential character of fluorescence decay.[26] However, broad absorption and fluorescence bands did not allow for an unambiguous spectral separation. Prompted by these results, we have undertaken a systematic supersonic jet laser-induced fluorescence studies of two substituted porphycenes with a small N−N distance: 9,10,19,20-tetra-*n*-methylporphycene (**1a**) and 9,10,19,20-tetra-*n*-propylporphycene (**1b**) (Chart 2). The results clearly show the existence of two differently absorbing and emitting species, which are assigned to trans and cis tautomeric forms. The spectra of both tautomers reveal splittings that disappear upon substitution of the internal hydrogen atoms with deuterium. The analysis of fluorescence excitation, population labeling scans, and dispersed fluorescence shows that the S_0−S_1 vibronic transitions occur between two slightly nonsymmetrical double minimum potentials. The asymmetry, which becomes reversed in S_1, is due to coupling of hydrogen movement with rotations of methyl groups. The values of the

(12) Smedarchina, Z.; Zgierski, M. Z.; Siebrand, W.; Kozlowski, P. M. *J. Chem. Phys.* **1998**, *109*, 1014.
(13) Wehrle, B.; Limbach, H. H.; Kocher, M.; Ermer, O.; Vogel, E. *Angew. Chem., Int. Ed. Engl.* **1987**, *26*, 934.
(14) Langer, U.; Hoelger, C.; Wehrle, B.; Latanowicz, L.; Vogel, E.; Limbach, H. H. *J. Phys. Org. Chem.* **2000**, *13*, 23.
(15) Waluk, J.; Müller, M.; Swiderek, P.; Köcher, M.; Vogel, E.; Hohlneicher, G.; Michl, J. *J. Am. Chem. Soc.* **1991**, *113*, 5511.
(16) Waluk, J.; Vogel, E. *J. Phys. Chem.* **1994**, *98*, 4530.
(17) Kyrychenko, A.; Herbich, J.; Izydorzak, M.; Gil, M.; Dobkowski, J.; Wu, F. Y.; Thummel, R. P.; Waluk, J. *Isr. J. Chem.* **1999**, *39*, 309.
(18) Sepioł, J.; Stepanenko, Y.; Vdovin, A.; Mordziński, A.; Vogel, E.; Waluk, J. *Chem. Phys. Lett.* **1998**, *296*, 549.
(19) Even, U.; Jortner, J. *J. Chem. Phys.* **1982**, *77*, 4391.
(20) Gil, M.; Jasny, J.; Vogel, E.; Waluk, J. *Chem. Phys. Lett.* **2000**, *323*, 534.
(21) Webb, L. E.; Fleischer, E. B. *J. Chem. Phys.* **1965**, *43*, 3100.
(22) Wu, Y. D.; Chan, K. W. K.; Yip, C. P.; Vogel, E.; Plattner, D. A.; Houk, K. N. *J. Org. Chem.* **1997**, *62*, 9240.
(23) Baker, J.; Kozlowski, P. M.; Jarzecki, A. A.; Pulay, P. *Theor. Chem. Acc.* **1997**, *97*, 59.
(24) Kozlowski, P. M.; Zgierski, M. Z.; Baker, J. *J. Chem. Phys.* **1998**, *109*, 5905.
(25) Vogel, E.; Köcher, M.; Lex, J.; Ermer, O. *Isr. J. Chem.* **1989**, *29*, 257.
(26) Gil, M.; Borowicz, P.; Dobkowski, J.; Marks, D.; Zhang, H.; Glasbeek, M.; Waluk, J. Manuscript in preparation.

tunneling splitting indicate that the vibrational wave functions of the inner hydrogen atoms are delocalized over the two minima in the ground state and much more localized in S_1, which is consistent with a larger energy barrier for tautomerization in the latter.

Experimental and Computational Details

9,10,19,20-Tetra-*n*-methylporphycene and 9,10,19,20-tetra-*n*-propylporphycene were synthesized and purified according to previously described procedures.[25] The experimental setup for laser-induced fluorescence (LIF) measurements has been described in details elsewhere.[18] Typically, the sample was heated to 520 K and expanded with a helium carrier gas at 3 atm stagnation pressure into the vacuum chamber. The fluorescence was excited by a home-built narrow band dye laser pumped by a Nd:YAG laser (Surelite I-10, Continuum) operating at 10 Hz. The dye laser, using a DCM dye (Lambdachrome LC6500), had a line width of <0.3 cm^{-1}. The average energy of laser pulses was about 30 μJ. LIF spectra were detected by a Hamamatsu R2949 photomultiplier using a Schott GG645 cutoff filter.

For two-color fluorescence depletion experiments,[18] a narrow band (<0.1 cm^{-1}) optical parametric oscillator (OPO, Sunlite EX, Continuum) was used, pumped by a seeded Nd:YAG laser (Powerlite Precision 8000, Continuum) as the second excitation source. The probe laser was fixed at the wavelength resonant with the electronic transition of the selected species. A typical delay between the pump and the probe pulses was about 220 ns.

To record dispersed fluorescence (DF) spectra, the fluorescence was collected by an optical system designed by Dr. Jan Jasny of the Institute of Physical Chemistry, Polish Academy of Sciences. The system consisted of two mirrors (toroidal and planar, respectively) that projected the fluorescence from the crossing region of the jet and the laser beam onto the entrance slit of an Acton SpectraPro275 spectrograph, equipped with a CCD camera (Princeton Instruments, Inc.) cooled by liquid nitrogen. For recording the fluorescence spectra in various ranges, 1200 and 1800 g/mm gratings of the spectrograph were used, the spectral resolution under these conditions being 9 and 5.5 cm^{-1}, respectively. To improve the signal-to-noise ratio, the data were accumulated within 10−30 min.

Deuteration of the sample was achieved either by passing the helium carrier gas through the reservoir containing D_2O or CH_3OD vapors or by dissolving the sample in a deuterated solvent in a dry helium environment and evaporating the solvent. Commercially available D_2O and CH_3OD (Dr. Glaser, AG Basel, isotopic purity 99.8 and 99.65%, respectively) were used.

The optimized geometries and vibrations were obtained by B3LYP/6-31G(d,p) calculations, as implemented in the Gaussian 2003 package of programs.[27] Electronic transition energies were computed using TD-DFT, with the same functional and the basis set.

Results and Discussion

Figure 1a shows the fluorescence excitation spectrum of **1a** seeded in supersonic free jet near the electronic origin of the $S_1 \leftarrow S_0$ transition. For comparison, the fluorescence excitation spectrum of parent, unsubstituted porphycene **1** is shown in Figure 1b. The observed transitions and the calculated vibrations are presented in Tables 1 and 2 for **1a** and **1**, respectively.

While in the case of the parent compound the electronic origin is split by 4.4 cm^{-1}, two bands lying 12.5 cm^{-1} apart, denoted as A (15 547.5 cm^{-1}) and B (15 560 cm^{-1}), are observed in the spectrum of **1a**. Each of these bands is split, in turn, into doublets separated by about 2 cm^{-1}. In contrast to the case of the parent porphycene, the spectrum of **1a** consists only of several low energy transitions: above 73 cm^{-1} from the strong B band no lines are detected in the fluorescence excitation.

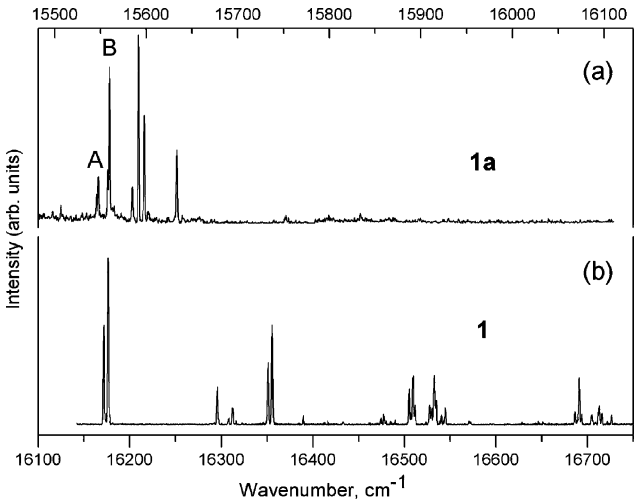

Figure 1. LIF excitation spectrum of **1a** (a) and the parent porphycene (b).

The complicated spectral structure near the electronic origin of **1a** has been investigated by double resonance fluorescence depletion experiments. The fluorescence dip spectra have been recorded with the probe laser set at the transitions observed at 15 558, 15 560, 15 592, and 15 598 cm^{-1}, respectively. For probing at 15 560 and 15 592 cm^{-1}, the spectra were recorded in the range of 15 540−15 750 cm^{-1} and they turned out to be identical. The spectra for probing at 15 558 and 15 598 cm^{-1} were recorded for shorter intervals, up to 15 610 cm^{-1}, where the main spectral features are present. The dips observed in the shorter scans revealed the same relative intensities and the same spectral positions as in the longer ones, suggesting that the four above-mentioned bands originate from the same level in the electronic ground state.

Figure 2 presents two fluorescence dip scans with the probe laser set at the lower and higher energy component of the B band doublet. Each of the scans shows two dips corresponding to both probed transitions. The two fluorescence dip scans are very similar and reveal many more dips than the number of transitions detected in the excitation spectrum. While the latter consists of single lines, almost all of the dips show doublet structure. A feature not detected in the excitation spectrum is revealed at 15 624 cm^{-1}, 64 cm^{-1} above the B origin, and many new dips that have no corresponding peaks in the excitation spectrum appear, starting from 85 cm^{-1} above the origin of the B band. A significant observation is that all features present in the excitation spectrum simultaneously appear in the hole-burning curves, indicating either a common origin or fast ground-state equilibration (<220 ns) between species responsible for A and B bands and their doublet components (labeled 1 and 2 in Figure 2). This behavior is completely different from that observed in **1**, where the components of the doublets were shown to arise from different ground-state origins.[18]

The relative intensities of the A and B bands in the fluorescence excitation spectrum depend on cooling conditions. The spectrum in Figure 2 was obtained while exciting the fluorescence 3 mm downstream from the nozzle. Increasing this distance and improving the conditions of cooling led to a complete suppression of the A band and the band lying 38 cm^{-1} higher (marked by the arrows, Figure 3). However, the rate of

(27) Frisch, M. J.; et al. *Gaussian 03, revision B.03*; Gaussian, Inc.: Pittsburgh, PA, 2003.

Table 1. Observed and Calculated Low Frequency Modes of trans and cis Tautomers of **1a**

1a trans[a]							**1a** cis[b]						
obsd (cm^{-1})				calcd (S_0)[c]		assignment	obsd (cm^{-1})				calcd (S_0)[c]		assignment
S_0 [d]		S_1 [e]					S_0 [d]		S_1 [e]				
		15558				0^{+}_{+}			15546				0^{+}_{+}
15560		15560				0^{-}_{+}	15548		15548				0^{-}_{+}
15546	14					0^{+}_{-}	15529	19					0^{+}_{-}
		15590	30			$1a_u{}^{+}_{+}$							
15528	32	15592	32	29	$1a_u$	$1a_u{}^{-}_{+}$					30	1a′	
15522	38	15598	38	38	$2a_u$	$2a_u{}^{-}_{+}$	15507	41	15576	38	37	1a″	$1a''{}^{+}_{+}$
15507	53					$2a_u{}^{+}_{-}$							
15497	63	15624	64	61	$1a_g$	$1a_g$					60	2a′	
		15632	72	73	$2a_g$	$2a_g$					74	2a″	
15482	78	15634	74	74	$3a_u$	$3a_u$					74	3a′	
15468	92	15658	98	97	$4a_u$	$4a_u{}^{+}_{+}$	15446	102			94	3a″	3a″
15543	107					$4a_u{}^{+}_{-}$							
15440	120												
15434	126	15688	128	130	$3a_g$	$3a_g$	15415	133			132	4a′	4a′
15419	141	15700	140	139	$4a_g$	$4a_g$					138	4a″	
15408	152	15719	159	157	$5a_g$	$5a_g{}^{+}_{+}$					154	5a″	
				160	$5a_u$		15388	160			157	5a′	5a′
				161	$6a_g$						157	6a″	
15392	168					$5a_g{}^{+}_{-}$							
15381	179			177	$6a_u$						176	6a′	
				206	$7a_g$		15353	195			205	7a″	
				208	$8a_g$						208	7a′	
				209	$7a_u$						209	8a″	
				217	$8a_u$						218	8a′	
15366	224			222	$9a_u$		15318	230			231	9a′	
15313	247			251	$9a_g$						251	10a′	
15292	268												
15275	285												
15253	307			316	$10a_u$						313	11a′	
				317	$10a_g$						320	12a′	
15230	330			330	$11a_g$						327	9a″	
15220	340			350	$11a_u$						345	10a″	
15194	366			359	$12a_u$		15198	350			358	11a″	
				378	$12a_g$						377	12a″	
15173	387			384	$13a_g$						384	13a′	
15162	398			403	$13a_u$						402	14a′	
				424	$14a_g$						423	13a″	
				430	$14a_u$						428	14a″	

[a] Assigned to form B. [b] Assigned to form A. [c] B3LYP/6-31G(d,p), cm^{-1}. [d] From dispersed fluorescence. [e] From fluorescence excitation and hole burning.

disappearance of the A band is much slower than that of the "normal" hot bands, observed to the red and to the blue from the A and B origins (marked by the asterisks, Figure 3). This result indicates that the suppression of A may involve a process other than vibrational cooling. Moreover, the A and B bands are thus due to transitions from different levels (species) in the ground state, which, however, communicate on the time scale shorter than 220 ns, as revealed by fluorescence depletion experiments. It should also be noted that the relative intensities of the two components of both A and B doublets do not change with cooling.

The attempts to record the fluorescence dip spectrum when probing the origin of the A transition were not successful. This transition is weaker than B, is "hot" in its nature, and is observable only under incomplete cooling conditions at the first stages of supersonic expansion. Under these conditions, a substantial amount of unresolved fluorescence background from the "hot" unrelaxed molecules is present. This reduces our effective resonant fluorescence dip signal. An important observation is that we were not able to observe the fluorescence dip spectrum when pumping into the B transition and probing the A band. On the contrary, when we pump from the ground-state level of A (15 547.5 cm^{-1}) and then probe the population of B level, we can see a small but reproducible dip (cf. probe 2 scan in Figure 2). Additionally, a dip corresponding to the 38 cm^{-1} mode of A is clearly observed at 15 585 cm^{-1}. These findings imply that the communication between A and B species is only one directional, from A to B, but not vice versa. The ground-state level of B is the lower one, and thus the possibility of preferential equilibration of A into B seems to be a reasonable explanation.

Both A and B systems reveal a low frequency mode of 38 cm^{-1}. On the contrary, the band with the frequency of 32 cm^{-1} relative to the B origin has no correspondence in the spectrum originating from the A band.

In principle, the complicated structure of the spectrum of **1a** could be due to the presence of different conformers related to different relative configurations of the four methyl groups. To determine whether the spectral structure is due to different conformers or rather is caused by changes in the chromophore geometry, and thus in the electronic properties of the porphycene skeleton, the excitation spectrum was recorded for the tetra-

Table 2. Observed and Calculated Frequencies for the trans Form of **1**

obsd (cm^{-1})[a]						
S_0 [c]		S_1 [d]		calcd (S_0)[b]		assignment
16175		16175				0^+_+
16170.6		16170.6				0^-_-
				60	$1a_u$	
				71	$2a_u$	
				87	$3a_u$	
				118	$1b_g$	
				136	$2b_g$	
16028	147	16311	136	150	$1a_g$	$1a_g$
15997	178	16354	179	187	$2a_g$	$2a_g$
				198	$3b_g$	
				206	$4a_u$	
		16388	213	209	$4b_g$	$4b_g$
				238	$1b_u$	
				311	$5a_u$	
				319	$6a_u$	
				324	$2b_u$	
15834	341	16508	333	347	$3a_g$	$3a_g$
15811	364	16531	356	371	$4a_g$	$4a_g$
				391	$3b_u$	
		16543	368	399	$5b_g$	$5b_g$
15694	481			492	$5a_g$	$5a_g$
15655	520	16689	514			$2a_g + 3a_g$
15633	542	16714	539			$2a_g + 4a_g$
				611	$6a_g$	
15508	667	16820	645	675	$7a_g$	$7a_g$
		16828	653			
15493	682					$2 \times 3a_g$
15470	705					$3a_g + 4a_g$
		16999	824	833	$8a_g$	
		17038	863	877	$9a_g$	
15209	966			989	$10a_g$	
15185	990			994	$11a_g$	
				1016	$12a_g$	
				1082	$13a_g$	
15115	1060			1092	$14a_g$	
				1142	$15a_g$	
15015	1160			1193	$16a_g$	
14973	1202			1240	$17a_g$	
14915	1260			1292	$18a_g$	
				1312	$19a_g$	
14839	1336			1370	$20a_g$	
				1387	$21a_g$	
				1413	$22a_g$	
14772	1403			1442	$23a_g$	
				1448	$24a_g$	
				1490	$25a_g$	
14697	1478			1533	$26a_g$	
14669	1506			1563	$27a_g$	
				1592	$28a_g$	
14608	1567			1613	$29a_g$	
14560	1615			1663	$30a_g$	

[a] Vibronic peaks corresponding to the higher energy component of the tunneling doublet. [b] B3LYP/6-31G(d,p), cm^{-1}; above 400 cm^{-1}, only a_g and b_g modes are shown. [c] From dispersed fluorescence. [d] From fluorescence excitation.

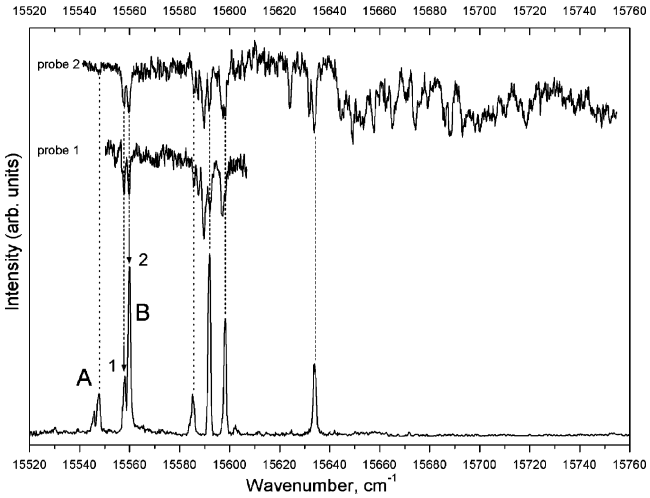

Figure 2. (Bottom) LIF excitation spectrum of **1a**. (Top) Fluorescence dip spectra with the probe laser set at 15 558 cm^{-1} (probe 1) and 15 560 cm^{-1} (probe 2).

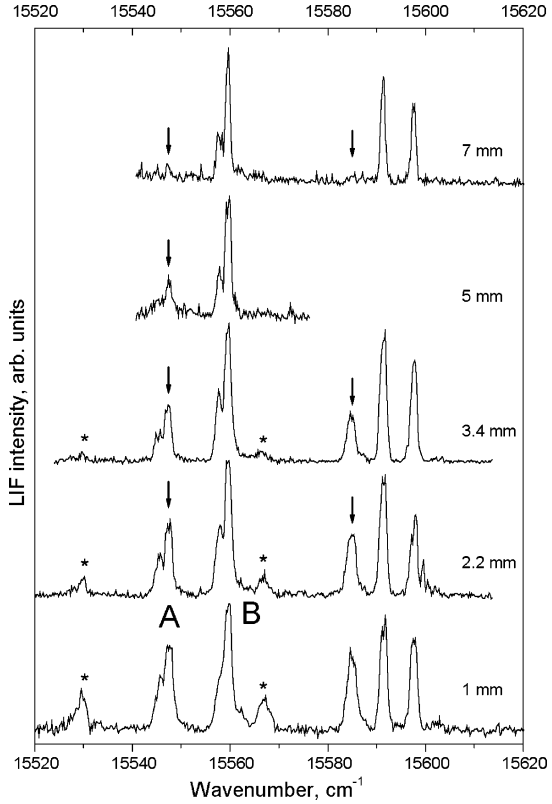

Figure 3. Relative intensities of the bands in the low energy part of the excitation spectrum of **1a** as a function of the distance between the nozzle and the laser beam. Hot bands are indicated by asterisks. Arrows show features due to form A, which disappear upon cooling.

propyl-substituted derivative **1b**, for which the X-ray data show that the inner cavity parameters are practically the same as those in **1a**. The spectra of **1a** and **1b** are very similar (Figure 4). The same basic pattern as observed for **1a**, two bands near the electronic origin, labeled A and B, is found also for **1b**. Similarly as in **1a**, each of both bands in **1b** reveals the splitting. The A and B components in **1b** are separated by ca. 17 cm^{-1}, compared to 12.5 cm^{-1} in **1a**. Two features of **1a**, separated by 32 and 38 cm^{-1} from the origin of band B, as well as the transition observed at 38 cm^{-1} from the origin of band A, have their counterparts in **1b**, although the intensity pattern is somewhat different. Similarly to the case of **1a**, no lines in the excitation spectrum were detected for **1b** in the region above 70 cm^{-1} from the position of the B band. We therefore conclude that the possible presence of various rotational conformers due to alkyl substituents is not the major factor responsible for the characteristics of the supersonic jet spectra of **1a** and **1b**.

It is known that the bridge alkyl substituents have a large impact on the spectral and photophysical properties of porphycene.[15,28] The former is reflected in the shape of the electronic absorption spectra in condensed phases. The bands corresponding to the origins of the S_0-S_1 and S_0-S_2 electronic

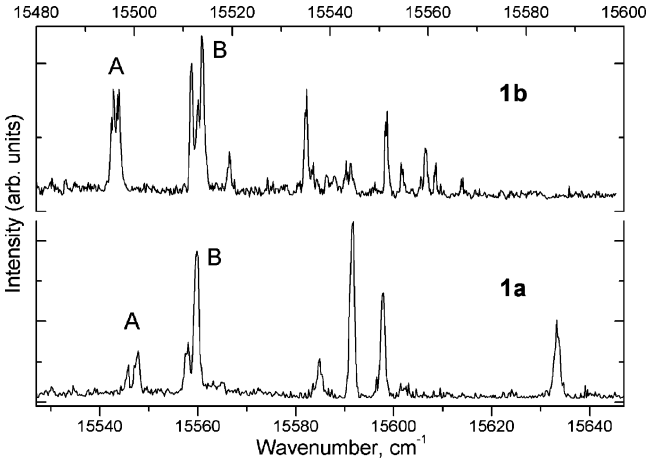

Figure 4. Fluorescence excitation spectrum of **1a** (bottom) and **1b** (top).

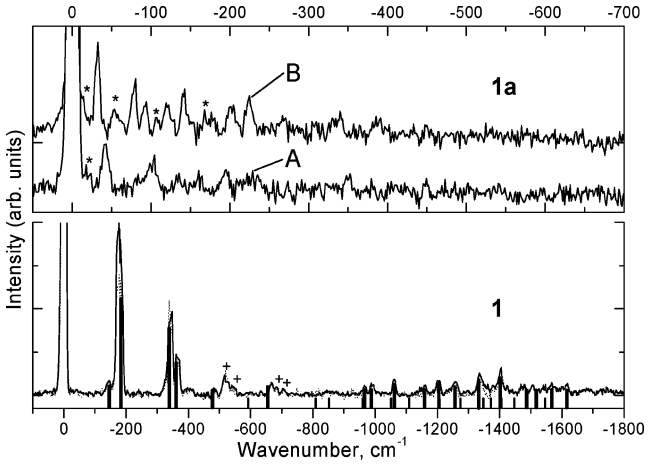

Figure 5. (Top) Dispersed fluorescence spectra of **1a** (B, excited at 15 560 cm^{-1} (form B); A, excited at 15 547.5 cm^{-1}(form A)). Asterisks mark the bands that cannot be associated with the calculated modes (see also Table 1). (Bottom) Spectra of the parent porphycene (solid line, excited at 16 175 cm^{-1}, dotted line, excited at 16 170.6 cm^{-1}). Crosses mark the positions of overtones and combination bands. Calculated positions of ground-state vibrations are also shown, with thicker bars indicating the assigned transitions. Calculated frequencies were scaled by a factor of 0.97.

transitions are well-separated, by about 900 cm^{-1}, in the parent molecule **1**,[29] while in **1a** and **1b** they strongly overlap. The influence of bridge alkyl substituents on the photophysical characteristics is even more spectacular: Fluorescence quantum yield in room temperature solutions drops by nearly 3 orders of magnitude with regard to that of the parent compound.[30] These effects are practically the same in **1a** and **1b**. The X-ray analysis of both molecules shows that the dimensions of the skeleton are roughly the same and quite different from those of the unsubstituted compound.[30] In particular, the distance between hydrogen-bonded inner cavity nitrogen atoms becomes much smaller (2.53 Å in both **1a** and **1b**, compared to 2.63 Å in the parent porphycene). As discussed below, these geometry changes, confirmed by calculations, may lead to significant stabilization of the cis versus trans tautomeric forms.

Figure 5 shows DF spectra of the parent porphycene and of **1a** excited into the A and B bands. In the case of porphycene, the DF spectra excited at 16 170.6 and 16 175 cm^{-1}, the two components of the tunneling doublet, are very similar. Vertical bars below the spectra denote the positions of a_g ground-state vibrations obtained from calculations. The results of calculations for **1** (Table 2) show very good agreement with experiment. The assignments are rather straightforward in the region below 1000 cm^{-1} and less so for higher frequency vibrations. Still, each of the observed peaks can be associated with its computational counterpart. The observed frequencies match nicely those reported in the studies in rare gas matrices.[29,31] Characteristically enough, only totally symmetric modes are observed in fluorescence.

Due to lower fluorescence efficiency in comparison with that of parent porphycene, the spectra for **1a** had to be recorded with lower spectral resolution to improve the signal-to-noise ratio. While the DF spectrum of **1a** excited at 15 547.5 cm^{-1} (band A) is weak, it certainly looks different from the DF spectrum obtained upon excitation into the band B, at 15 560 cm^{-1}. For instance, the 38 cm^{-1} vibrational mode is clearly seen in the band A spectrum, while the band B spectrum is dominated by the mode with the frequency of 32 cm^{-1}. The most striking feature in the fluorescence from B is the presence of several peaks in the range below 170 cm^{-1} that cannot be correlated with any calculated low frequency modes. The first of these peaks is located 14 cm^{-1} from the origin, whereas the calculations predict the lowest frequency mode of the trans tautomer at 29 cm^{-1}, in agreement with the peak observed at 32 cm^{-1}. Characteristically enough, other peaks that do not have their calculated counterparts are red-shifted by approximately the same amount, 15−16 cm^{-1}, from the observed (and calculated) bands (Table 1). Such behavior, revealed by at least three more pairs, 38−53, 92−107, and 152−168 cm^{-1}, can be the manifestation of tunneling splitting in the ground state of **1a**.

It was shown previously that the splitting of the electronic origin and the vibronic features observed in the fluorescence excitation spectra in parent porphycene are related to the ground-state double hydrogen tunneling.[18] The crucial criterion in studying the tunneling is the response of the system to the replacement of the protons by deuterons. The sample of **1a** was deuterated in situ by dissolving in D_2O and further evaporation of the solvent. The D_2O vapors with partial pressure of ∼0.1 torr were added into the expansion mixture to suppress the reverse exchange of the deuterium into hydrogen. The resulting spectrum is presented in Figure 6 (top). Upon deuteration, new bands appear at the red side of the spectrum. Similar spectra (absolute band positions) have been obtained using CH_3OD as the deuteration agent. The dependence of intensity on the partial pressure of the deuteration agent enabled the assignment of the bands at 15 401 and 15 409.5 cm^{-1} to the origins of doubly deuterated (ND,ND) forms, and the bands at 15 460 and 15 470 cm^{-1} to the origins of a singly deuterated (NH,ND) forms. The intensity of the A″ and A′ bands at 15 401 cm^{-1} and 15 460 cm^{-1} relative to their doublet counterparts B″ and B′, respectively, depends on the conditions of cooling. At higher distances between the nozzle and the excitation laser beam these origins and the corresponding vibronic bands disappear from the spectrum, thus resembling the A origin band of undeuterated **1a**. The separations between the A and B origins are slightly

(28) Levanon, H.; Toporowicz, M.; Ofir, H.; Fessenden, R. W.; Das, P. K.; Vogel, E.; Kocher, M.; Pramod, K. *J. Phys. Chem.* **1988**, *92*, 2429.
(29) Starukhin, A.; Vogel, E.; Waluk, J. *J. Phys. Chem. A* **1998**, *102*, 9999.
(30) Gil, M.; Urbańska, N.; Luboradzki, R.; Pietraszkiewicz, M.; Waluk, J. Manuscript in preparation.
(31) Malsch, K.; Hohlneicher, G. *J. Phys. Chem. A* **1997**, *101*, 8409.

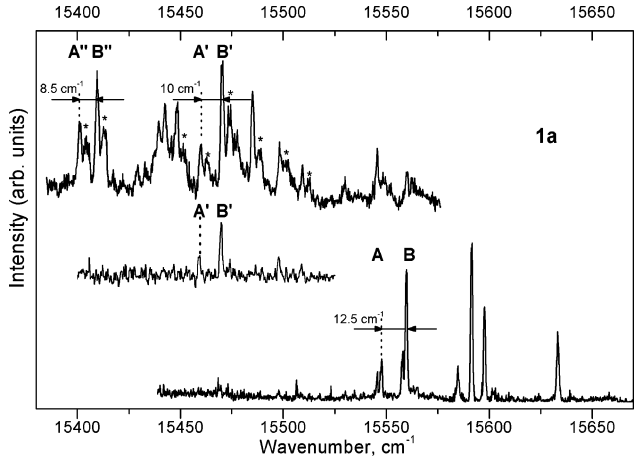

Figure 6. LIF excitation spectra of **1a**. Top, deuterated; bottom, nondeuterated species; and middle, results for deuterated sample measured without the presence of deuterating agent in the beam. Bands assigned to complexes with D_2O are marked by asterisks. Primed and double primed features correspond to uncomplexed, singly, and doubly deuterated species, respectively.

lower for deuterated samples, amounting to 10 cm^{-1} for singly deuterated and 8.5 cm^{-1} for doubly deuterated **1a**. Some spectral features lying to the blue from the origins of A and B bands in the deuterated forms vary in intensity with D_2O concentration and are therefore assigned to complexes with D_2O (marked by the asterisks in Figure 6). To distinguish the spectra due to complexes from those of the uncomplexed deuterated molecule, experiments were also performed without adding the deuteration agent to the expansion mixture, while using the sample deuterated prior to measurements. The middle part of Figure 6 shows the spectrum for an (NH,ND) form of **1a** free from the complexes. The crucial observation is that the doublet structure is no longer observed in both A and B origins. The same is true for the doubly deuterated (ND,ND) form.

Upon deuteration, the spectra move to the red, indicating that the shifts of the vibrational levels in the deuterated species are larger in S_1 than in S_0. This, in turn, implies that the intramolecular NH···N hydrogen bond is weaker in the excited state. Thus, tunneling splitting in S_1 can be expected to be smaller than that in S_0. Similar behavior was observed in parent porphycene. Other spectral characteristics, however, are completely different for the parent compound, on one hand, and for both **1a** and **1b**, on the other. In the former, both lower and upper components of the ground-state tunneling doublet of the trans tautomer could be selectively excited. No evidence was found in **1** for the presence of cis forms. In **1a** and **1b**, the excitation originates from a common level, which, as shown by fluorescence depletion scans, is populated from two different species, A and B, one of which disappears upon cooling. Both forms exhibit similar shifts in transition energy after deuteration. We assign the A and B bands to different tautomeric species, cis and trans, respectively. The form of which the intensity is reduced upon cooling corresponds to the higher energy structure. The calculations (Table 3) predict that in the ground state the trans species should be energetically lower, although the difference is very small, the cis form being higher in energy by only 0.69 kcal/mol. For the parent porphycene, the cis−trans energy difference is calculated as 1.6 kcal/mol. A very similar value, 1.9 kcal/mol, has been obtained for **1** using 6-31G(d) and an a large triple-ζ double polarization (TZ2P) basis set.[24]

Table 3. Results of B3LYP/-31G(d,p) Calculations for **1a** and Parent Porphycene **1**[a]

	ΔE (cis–trans)[a]	E (TS) [a]	E (SS) [a]
1a	1.40 (0.69)	2.41 (−0.51)	3.62 (−1.60)
1	2.23 (1.6)	4.10 (1.01)	6.10 (0.59)

[a] Calculated energy differences (kcal/mol) between the ground state cis and trans, trans−cis transition states (TS), and trans−trans second-order saddle points (SS). [b] In parentheses: energies including zpve correction

Comparison of **2**, **1**, and **1a** reveals that the two tautomeric species are getting closer in energy as the distance between hydrogen-bonded nitrogen atoms becomes smaller. This is understandable, because upon compressing the hydrogen bonds, both forms are approaching a symmetric structure, with the hydrogen equidistant from two nitrogen atoms.

For the undeuterated species, both A and B bands consist of doublets, of which the intensity does not change upon cooling. This doublet structure disappears in singly and doubly deuterated molecules, suggesting that its origin may be due to tunneling. Since both components of the doublet originate from the same ground-state level, their separation, about 2 cm^{-1}, has to be assigned to the tunneling splitting in the S_1 state. In porphycene, we postulated that the splitting in S_1 is much lower than the value of 4.4 cm^{-1}, corresponding to the ground state. Since in both **1a** and **1b** the NH−N distance is significantly smaller than that in the parent molecule, a stronger hydrogen bond is expected, which should lead to smaller barriers and larger tunneling splittings in both S_0 and S_1. The barriers can be estimated from the molecular geometries and the ground-state splitting value of 4.4 cm^{-1} in parent porphycene. A simple one-dimensional model[32,33] yields the formula that relates the double hydrogen tunneling splitting ΔE to the barrier height V, barrier width d, and the effective mass m:

$$\Delta E = \frac{h\nu}{\pi}\exp\left[-\frac{\sigma d}{\hbar}\sqrt{2m(V-E_0)}\right] \qquad (1)$$

σ is the shape parameter, usually close to unity and equal to $\pi/4$ for parabolic barriers. Because of the lack of experimental assignment for the NH stretching vibration, the vibrational frequency ν has to be estimated. Due to the highly anharmonic potential for the hydrogen motion, the value of ν can be much lower than that expected for the NH stretching vibration. Indeed, while the calculations for **1** predict a strong IR band (the most intense of all IR-active transitions) at 2890 cm^{-1}, no significant absorption has been detected in this region.[31] It should be stressed that the value below 3000 cm^{-1} obtained for the NH stretching mode in the harmonic approximation is already suggesting a very strong hydrogen bond. For the trans and cis tautomers of **1a**, our calculations yield even lower values, 2653 and 2420 cm^{-1}, respectively.

To estimate the value of ν, we use the formula obtained for tunneling in symmetrical double minimum potentials via a harmonic oscillator approximation:[34]

$$\Delta E = \frac{h\alpha^{3/2}d}{2m\pi^{5/2}}\exp(-\alpha d^2) \qquad (2)$$

(32) Bell, S.; Crayston, J. A.; Dines, T. J.; Ellahi, S. B. *J. Phys. Chem.* **1996**, *100*, 5252.
(33) Trommsdorff, H. P. *Adv. Photochem.* **1998**, *24*, 147.
(34) Harmony, M. D. *Chem. Phys. Lett.* **1971**, *10*, 337.

where $\alpha = 2\pi m\nu/\hbar$. For the parent porphycene, using the experimental value of ground-state tunneling splitting, 4.4 cm^{-1}, and varying m between 1 and 2 and d between 0.55 and 0.65 Å (tunneling distance estimated from the X-ray data[2] is 0.60 Å) yields values of ν ranging between 185 and 673 cm^{-1}. These values, in turn, result in the estimated barrier heights of 217−1360 cm^{-1} (2.6−16.0 kJ/mol). In **1a** and **1b**, one expects the decrease of d by about 0.1 Å (the NH−N distances are 2.63, 2.53, and 2.53 Å in **1**, **1a**, and **1b**, respectively). Since the hydrogen bond strength depends on this distance, it should increase in alkylated derivatives. Therefore, the tautomerization barrier should decrease. Using eq 1, we predicted about a 2-fold increase in tunneling splitting for the decrease in nitrogen separation by 0.1 Å and the reduction of V by 10−20%.

While the increase in hydrogen-bonding strength in **1a** and **1b** certainly lowers the barrier to hydrogen transfer, the 4-fold alkyl substitution may lead to asymmetric potentials and smaller proton flux through the barrier. Coupling between proton transfer in a double well potential and rotation of the methyl group has been thoroughly studied for molecules such as α-methyl-β-hydroxyacrolein,[35] tropolone,[36] and hydroxyphenalenone.[37,38] Depending on the relation between time scales for proton oscillation on one hand, and methyl rotation on the other, two cases can be distinguished. When the proton transfer is very fast the potential along the proton-transfer coordinate remains symmetric and the methyl substitution does not much influence the tunneling rate. In the asymmetric coupling case, the proton transfer is slower. Such a situation may lead to an asymmetric potential for the proton transfer and lowering of the tunneling rate. For the ground state of methyl-substituted tropolone and 9-hydroxyphenalenone, the borderline between the two coupling regimes has been estimated as occurring for proton tunneling times lying in the range of 240−790 fs.[38]

In the parent porphycene, the ground-state tunneling time based on the 4.4 cm^{-1} splitting is about 2 ps. As discussed below, the decrease of d from 0.60 to 0.50 Å should shorten this value approximately by a factor of 2.

The loss of inversion symmetry in **1a** and **1b** can explain the features observed in the fluorescence excitation and hole-burning spectra of the two molecules. Both components of the doublet structure that we assign to tunneling splitting in S_1 appear in the same hole-burning spectrum, contrary to the case of the parent porphycene. In other words, transitions are observed in **1a** from the lower energy component of the tunneling doublet in S_0 to both components in S_1. This may be understood if the inversion symmetry is present in **1**, but not in **1a**. For the latter, the selection rule allowing only transitions between states of the same parity no longer applies, and both +,− and −,+ transitions become allowed.

A confirmation of the lower symmetry in **1a** is provided by the analysis of vibronic features observed in the fluorescence excitation spectrum. The calculations predict C_i symmetry for the trans tautomers and C_s symmetry for the cis forms of **1a** (in the latter, the vertical symmetry plane is perpendicular to the plane of the molecule). The calculated S_1 and S_2 electronic states

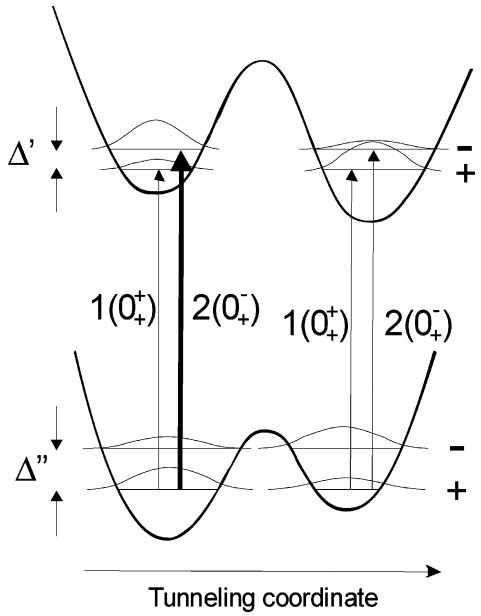

Figure 7. Scheme of S_0 and S_1 potential energy surfaces and the resulting transitions. Δ″ and Δ′ denote ground- and excited-state tunneling splittings, respectively.

are of A_u symmetry in the trans tautomer. For the cis form, two close-lying singlet states are predicted in the low energy region, their symmetry species being A′ and A″, respectively. This corresponds to the transition moment from the ground state polarized along the vertical (A′) or horizontal (A″) in-plane molecular axis.

Tables 1 and 2 show the comparison between the calculated and observed low frequency modes for both tautomeric forms of **1a** and the corresponding values for the parent porphycene. In the latter, only vibrations of allowed *gerade* symmetry appear both in absorption and emission. On the contrary, the tetramethyl derivative reveals transitions that should belong to the a_u species, forbidden in a centrosymmetric molecule.

Very good correspondence is preserved between the S_0 vibrational frequencies observed in the emission and those of S_1 detected by fluorescence excitation/hole burning. However, we also detect features that are only observed in emission. For excitation into the B band, this is a weak band lying 14 cm^{-1} to the red from the origin and three peaks observed 15−16 cm^{-1} to the red of the peaks that have their counterparts in absorption. In the case of excitation into A, we find a corresponding feature 19 cm^{-1} to the red of the origin band in the fluorescence spectrum. We assign these features, indicated by asterisks in Figure 5, to (+,−) transitions ending on the higher level of the ground-state tunneling splitting doublets. The ground-state splittings are much larger than the separation of 2 cm^{-1} between the components 1 and 2 of the A and B doublets, observed in both fluorescence excitation and hole burning spectra and attributed to the splitting in S_1. This is consistent with red shifts obtained upon deuteration, which indicate that the hydrogen bonding is weaker in S_1, and thus the barrier for tautomerization is larger.

The model that explains all the features observed in the spectra is that of an asymmetrical double minimum potential for hydrogen transfer, with the relative energy ordering of the minima reversed in S_1 (Figure 7). The reversal occurs because the configuration of methyl groups is different in S_0 and S_1.

(35) Busch, J. H.; Fluder, E. M.; de la Vega, J. R. *J. Am. Chem. Soc.* **1980**, *102*, 4000.
(36) Nishi, K.; Sekiya, H.; Kawakami, H.; Mori, A.; Nishimura, Y. *J. Chem. Phys.* **1999**, *111*, 3961.
(37) Busch, J. H.; de la Vega, J. R. *J. Am. Chem. Soc.* **1986**, *108*, 3984.
(38) Nishi, K.; Sekiya, H.; Mochida, T.; Sugawara, T.; Nishimura, Y. *J. Chem. Phys.* **2000**, *112*, 5002.

Due to larger ground-state population and favorable Franck−Condon factors, the higher energy component of the doublet originating, in the absorption, from the lowest ground-state level should be more intense than its lower energy counterpart. Since the ground-state separation exceeds 10 cm^{-1}, the population of the upper component of the ground-state tunneling doublet should be much lower than that in the parent porphycene, where the separation of the levels is 4.4 cm^{-1}. One should also note that, due to the presence of four alkyl groups, the relaxation from the upper tunneling level should be much more effective than that in the unsubstituted molecule. These arguments explain the lack of detectable population of the upper component of the ground-state tunneling doublet. We note, though, that we observe hot bands while detecting the fluorescence at short distances from the nozzle. The band at 15 530 cm^{-1} (indicated by asterisk in Figure 3) may well correspond to the transition from the upper tunneling level of the A form. The corresponding feature for the B form may be hidden under the origin of the A band.

Strictly speaking, in the case of asymmetric potentials the term "tunneling splitting" loses its exact meaning, and the values of the splittings should be considered as upper limits to those expected for an ideal symmetric double minimum. However, because the wave functions seem to be delocalized, the asymmetry cannot be large, at least for the ground state. In general, localization of the wave functions becomes significant when one of the wells is stabilized by an amount comparable to the value of the tunneling splitting in the parent symmetrical system.

We have also measured the lifetimes of fluorescence upon exciting both components of the tunneling doublet in both A and B. The shorter lifetimes were obtained for the lower energy components (12.5 versus 17.3 ns for the fluorescence excited into 1 and 2 in A, respectively, 14.4 versus 19.3 ns for the corresponding values in B). This is consistent with the fact that, in a symmetric case, the lower energy transition (+,+) is allowed, while the latter (−,+) is forbidden.

Another intriguing feature of the LIF spectra of both **1a** and **1b** is the onset of efficient radiationless relaxation at very low excitation energy excess. We attribute it to the proximity of two electronic states, suggested already on the basis of experiments performed for **1b** in solutions and polyethylene films.[26] Also, the TD-DFT calculations for **1a** predict the S_1 and S_2 $\pi\pi^*$ levels to lie very close, 520 cm^{-1} in the cis structure and 821 cm^{-1} in the trans tautomer. For **1**, the calculations, performed on the same level, give the value of 981 cm^{-1}. The two states, interacting via a *pseudo*-Jahn−Teller effect, can significantly distort the potential energy curve of the lower level, thus providing a channel of rapid deactivation to the ground state. Since the fluorescence quantum yields of both **1a** and **1b** in solution are extremely sensitive to viscosity, the state coupling probably involves a large-amplitude distortion of the molecular skeleton, hindered in a rigid environment, but still occurring in a cold, isolated molecule. An interesting feature revealed in the jet is that in the region of low energy vibrations only one of the tunneling doublet components is connected with a rapid deactivation channel. This is seen upon comparing the fluorescence excitation spectra with the hole-burning scans (Figure 2). Both components are seen in the latter, but the fluorescence is observed only while exciting one of them. The symmetry seems to play a major role, as evidenced by the behavior of the deuterated species. In a singly deuterated **1a**, the intense peak observed at 32 cm^{-1} from the B origin practically disappears; it is recovered again in the doubly deuterated species (Figure 6). The same vibration provides the strongest fluorescence excitation peak in **1a**, whereas in **1b** its intensity is rather weak (Figure 4). To elucidate the mechanism of efficient radiationless deactivation in bridge-substituted porphycenes, extensive studies are carried out in our laboratory.[26,30] The initial results show that the deactivation channel involves direct relaxation to S_0 and that the process, at least in condensed phases, is not dependent on the deuteration of the inner hydrogen atoms.

Summary

The results obtained for two alkylated porphycenes **1a** and **1b** provide arguments for the presence of cis and trans tautomers of comparable ground-state energies. This observation, consistent with our findings in solutions, glasses, and polymer films[26] is also confirmed by calculations, which demonstrate that the decrease of the NH···N distance brings the energies of the two forms into near degeneracy.

Both tautomers reveal double hydrogen tunneling splitting of similar magnitude, which is understandable, given their similar energies and the inner cavity size. The splitting is larger than that in the parent compound, by the factor that is in agreement with simple considerations based on a one-dimensional model. As was the case for the parent porphycene, the barrier to tautomerization increases upon excitation. We attribute this to the expansion of the inner cavity in S_1. Excited-state optimizations are now in progress to test this hypothesis. Indeed, initial TD-DFT B-P86/TZVP geometry optimizations for **1** yielded 2.64 and 2.68 Å as the distance between hydrogen-bonded nitrogen atoms in S_0 and S_1, respectively. Interestingly, in the systems investigated thus far that exhibit tunneling splitting due to proton transfer, the barrier was lower in the excited state. Such was the case of tropolone,[39−50] its derivatives,[36,38,51−56] and hydroxyphenalenones.[38,57,58]

The role of alkyl substituents is crucial in many respects. First, by changing the electronic structure of the parent

(39) Alves, A. C. P.; Hollas, J. M. *Mol. Phys.* **1972**, *23*, 927.
(40) Alves, A. C. P.; Hollas, J. M. *Mol. Phys.* **1973**, *25*, 1305.
(41) Redington, R. L.; Redington, T. E. *J. Mol. Spectrosc.* **1979**, *78*, 229.
(42) Rosetti, R.; Brus, L. E. *J. Chem. Phys.* **1980**, *73*, 1546.
(43) Tomioka, Y.; Ito, M.; Mikami, N. *J. Phys. Chem.* **1983**, *87*, 4401.
(44) Alves, A. C. P.; Hollas, J. M.; Musa, H.; Ridley, T. *J. Mol. Spectrosc.* **1985**, *109*, 99.
(45) Redington, R. L.; Chen, Y.; Scherer, G. J.; Field, R. W. *J. Chem. Phys.* **1988**, *88*, 627.
(46) Sekiya, H.; Nagashima, Y.; Nishimura, Y. *Bull. Chem. Soc. Jpn.* **1989**, *62*, 9.
(47) Sekiya, H.; Nagashima, Y.; Nishimura, Y. *Chem. Phys. Lett.* **1981**, *160*, 581.
(48) Sekiya, H.; Nagashima, Y.; Nishimura, Y. *J. Chem. Phys.* **1990**, *92*, 5761.
(49) Sekiya, H.; Nagashima, Y.; Tsuji, T.; Nishimura, Y.; Mori, A.; Takeshita, H. *J. Phys. Chem.* **1991**, *95*, 10311.
(50) Paz, J. J.; Moreno, M.; Lluch, J. M. *Chem. Phys.* **1999**, *246*, 103.
(51) Sekiya, H.; Takesue, H.; Nishimura, Y.; Li, Z.-H.; Mori, A.; Takeshita, H. *J. Chem. Phys.* **1990**, *92*, 2790.
(52) Tsuji, T.; Sekiya, H.; Nishimura, Y.; Mori, A.; Takeshita, H. *J. Chem. Phys.* **1991**, *95*, 4802.
(53) Tsuji, H.; Sekiya, H.; Nishimura, Y.; Mori, R.; Mori, A.; Takeshita, H. *J. Chem. Phys.* **1992**, *97*, 6032.
(54) Ensminger, F. A.; Plassard, J.; Zwier, T. S. *J. Phys. Chem.* **1993**, *97*, 4344.
(55) Ensminger, F. A.; Plassard, J.; Zwier, T. S.; Hardinger, S. *J. Chem. Phys.* **1993**, *99*, 8341.
(56) Frost, R. T.; Hagemeister, F.; Schleppennach, D.; Laurence, G.; Zwier, T. S. *J. Phys. Chem.* **1996**, *100*, 16835.
(57) Rosetti, R.; Haddon, R. C.; Brus, L. E. *J. Am. Chem. Soc.* **1980**, *102*, 6913.
(58) Rosetti, R.; Rayford, R.; Haddon, R. C.; Brus, L. E. *J. Am. Chem. Soc.* **1981**, *103*, 4303.

porphycene, they lead to a smaller separation between nitrogen atoms, and thus to a stronger hydrogen bond. This situation results also in very close energies of the trans and cis tautomers, which allow the latter to be observed for the first time, even under conditions of cold, isolated molecules.

While strengthening the hydrogen bonds, the alkyl groups can simultaneously act against hydrogen tunneling, by slightly destroying the symmetry of the double minimum potential. The lower symmetry is reflected in the spectra by the appearance of modes that otherwise could not have been observed.

Finally, the presence of two nearby states in the alkylated derivatives results in rapid quenching of the emission. In this respect, the molecules in the jet resemble those in solutions of low viscosity (i.e., conditions that allow deactivation via large-amplitude motions).

The model presented in this work for double hydrogen tunneling did not address a possible role of those vibrations that do not necessarily involve hydrogen displacement, but can affect the tunneling potential, for instance by changing the distance between the hydrogen-bonded nitrogen atoms. Such an approach can be justified by the finding that the tunneling splittings observed for various vibronic bands do not seem to be much different from the splitting of the 0−0 transition. However, in unsubstituted porphycene there appears to be at least one exception, a transition observed at 178 cm^{-1} in S_0 and at 179 cm^{-1} in S_1, for which the splitting seems to be larger. This mode corresponds to a vibration that modulates the NH−N separation and thus can change the potential barrier for tautomerization. In consequence, a more accurate description of hydrogen tunneling in porphycenes may require extension to a multidimensional model.

If our synthetic plans succeed, the strategy for the future will be to study singly and doubly appropriately substituted porphycene derivatives. A smaller number of substituents should allow treating the problem of coupling between hydrogen motion and rotation of methyl groups in a more accurate, analytical fashion. Other plans predict emission measurements under conditions of even lower temperatures (helium droplets), which should lead to a more precise determination of tunneling splitting parameters in S_0 and S_1 states. On the theoretical side, both excited-state optimizations and quantum dynamic studies of tautomerization are underway.

Acknowledgment. This work was partially supported by Grant 3T09A 113 26 from the Polish Committee for Scientific Research and by the EC Grant G5MA-T-2002-04026.

Supporting Information Available: Complete ref 27. This material is available free of charge via the Internet at http://pubs.acs.org.

JA054745M